Fluorine Implantation and Residual Stresses in Polysilicon Films

Lynn Lowry
Jet Propulsion Laboratory
4800 Oak Grove Drive
Pasadena, CA 91109-8099

Paul Zschack
ORISE-Brookhaven National Laboratory
Upton, NY 11973-5000

Robert De Angelis
University of Nebraska-Lincoln
Center for Materials Research and Analysis
Lincoln, NE 68588-0656

ABSTRACT:

As microelectronic device dimensions are reduced below one micron, the hot carrier effect is a major barrier to continued scaling and VLS 1 reliability. Several reports have shown that fluorine diffusion into the device gate greatly enhances the resistance to hot carriers.(1 ,2,3) There has been some disagreement as to the mechanism of influence; however, several reports have suggested that the polysilicon is physically modified by the fluorine implant and that the beneficial effects are at least in part due to stress relaxation in the polysilicon.(1 ,3)

X-ray diffraction analysis was utilized to study the film stress effects in samples with various processing conditions. The sample matrix consisted of three thicknesses of polysilicon deposited on <100> silicon with a 25nm layer of SiO_2. The polysilicon was doped with phosphorous and arsenic after which the samples were implanted with fluorine at 30KeV at a dose of $6X10^{15}cm^2$. The polysilicon film stresses were evaluated by the powder diffraction technique which is routinely used to measure stress in polycrystalline material with a synchrotrons radiation source at Brookhaven National Laboratory on beamline X-14. X-ray rocking curve experiments were employed to determine the stress in the film from measurements of the curvature of the substrate. These two stress measurements are employed here to estimate the stress gradient in the intermediate amorphous oxide layer and correlations are made with the fluorine distribution in the wafer and the electrical characteristics of the structures.

INTRODUCTION:

As the dimensions of a device are reduced but the supply voltage remains constant the electric field generated in the silicon increases. These intensified electric fields can make it possible for electrons in the channel of the transistor to gain sufficient energy to be injected into the gate oxide. The charging of the gate oxide causes a long term device degradation. This process is exacerbated by the presence of dangling bonds at the silicon/oxide interface and/or bond strains and /or single charged impurity ions incorporated into the structure. Two possible methods to reduce these harmful effects is by reducing the stress existing in the structure or by

neutralizing the dangling bonds. implantation of ions, such as ^{19}F, into the silicon/oxide interface has the potential of both reducing the stress and elimination of the existing dangling bonds, thus reducing the detrimental hot carrier effects (4).

Ion implantation is used regularly in the fabrication of silicon based integrated circuits, However, there is still a considerable lack of knowledge concerning the effects of the damage on the structure of the device. Bai and Nicolet (S) have shown that ion implantation into <100> silicon produces a expansion strains, of the order of one percent, in the direction normal to the surface. The strains parallel to the surface are zero. This condition essentially transforms the silicon to a tetragonal structure with an expanded c axis normal to the (001) wafer surface. This effect is expected to occur in polycrystalline silicon at an fluorine ion doseof6E15 $/cm^2$(6).

EXPERIMENTAL METHODS:

Wafer Processing

The following strategies were employed in thc processing of the 380 micron thick silicon, (100) p-type doped wafers. A 25nm thick gate oxide layer was grown onto the basic wafer using diluted steam at 825C. A polysilicon layers of either 270, 480 and 830 nm were deposited onto the amorphous silica employing a substrate temperature of 625C. The polysilicon was doped with $POCL_3$ dopant was accomplished by P_2O_5 by gas deposition. The arsenic dopant was implanted at a total flux of 2X 10^{15} ions/cm^2 at 60KeV. The structures were annealed at 900C. Fluorine implantation of $6X10^{ls}$ was done at 30KeV and the structures were annealed at 900C. Secondary ion mass spectroscopy was employed to determine the depth profile of the silicon, the fluorine and the dopant concentrations through the layered structure.

TABLE I: Wafer Processing Characteristics

DOPANT ATOM TYPE	POLYSILICON THICKNESS (rim)	SiO_2 THICKNESS (rim)	FLUORINE ION DOSE (cm^2)
As	480	25	NONE
As	480	25	6E15
As	270	25	NONE
As	270	25	6E15
$POCl_3$	830	25	None
$POCl_3$	830	25	6E15
$POCl_3$	270	25	NONE
$POCl_3$	270	25	6E15
NONE	480	25	NONE

The wafer structures reported on in this investigation along with their processing characteristics are summarized in TABLE 1.

Synchrotron Measurements

The X 14 beamline at NSLS at Brookhaven National Laboratory was employed to determine the strains in both the random textured $POCL_3$ doped and the heavily [001] textured arsenic doped polysilicon films. The strains were converted to stresses using the method described by Flinn and Chiang (7). 'I'he x-ray profiles that were employed for Fourier shape analysis to determine the average diffracting particle size and the particle size distribution functions using the single order method reported by De Angelis et al.(8,9).

X-Ray Rocking Curve Measurements

An x-ray rocking curve system, described by Vreeland et al. (1 0,11) was employed to determine the curvature of the substrate. The curvatures were determined by measuring the change in the Bragg angle as a function of the horizontal translation of the wafer. The translation vector is normal to the diffraction vector. The radius of curvatures of the wafers were determined from the relationship; R= dS/d(Theta); where S is the value of the horizontal shift and theta is the Bragg angle for the (400) reflection. 'I'he stresses in the films were calculated from the substrate curvature following the method reported by Stoney (12) and discussed by Noyan and Goldsmith (13).

Electrical Measurements

On-state hot carrier stressing was performed on one micron fluorinated and control (non-fluorinated) nMOSFETs at $V_d=8.0V$, $V_g=3.0V$ (for maximum I_{sub}), and $V_{sub}=V_s=0V$. The devices were characterized before stressing and within a few minutes after 'stressing at room temperature and boiling liquid nitrogen temperatures.

RESULTS ANI) IlISCUSS]ON:

Polysilicon Microstructure

Cross sectional specimens were prepared for transmission electron microscope (TEM) observation of the microstructure developed in the processing. The $POCl_3$ doped polysilicon - shows a non-columnar, random grain structure, as can be seen in the micrographs in Fig, 1. However the grain structure of the arsenic doped samples,also shown in Fig. 1, was columnar and highly oriented in the [001] direction of growth. The degree of preferred orientation was determined from comparisons of standard theta-two theta intensities with the reported intensities of a random standard sample.

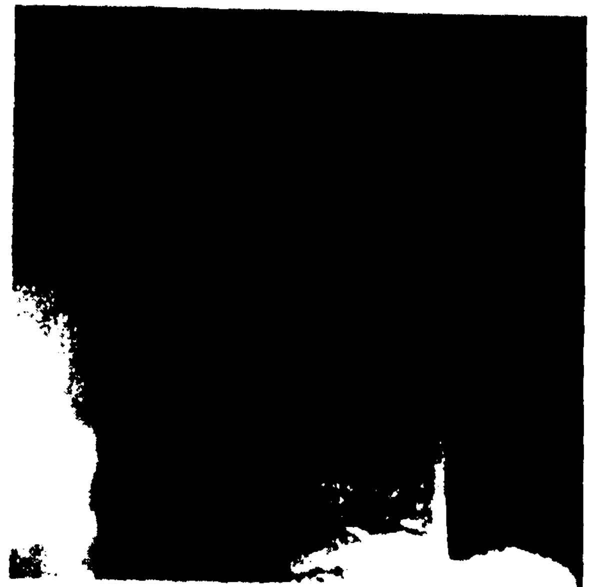

POCL DOPED **As IMPLANT**

Figure 1. Transmission Electron Micrographs of the Cross-Sections of the Processed Structures.

Secondary ion mass spectroscopy was employed to characterize the polysilicon dopant/implant compositional profiles through the layered structures. The fluorine compositional profile for the $POCl_3$ and the arsenic doped specimens, shown in Fig. 2, indicate that the fluorine concentration is about the same in the polysilicon. The notable differences are the arsenic implant has a large fluorine concentration gradient through the oxide layer and shows a minima fluorine diffusion into the single crystal substrate.

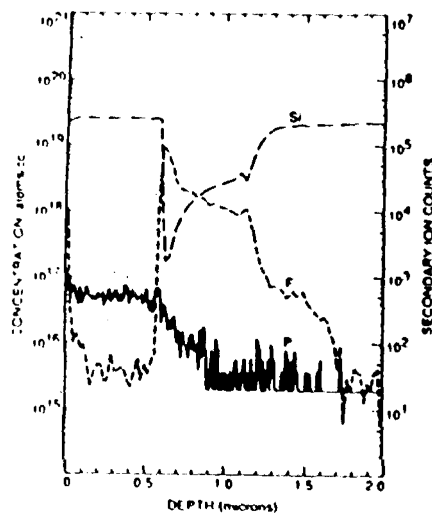

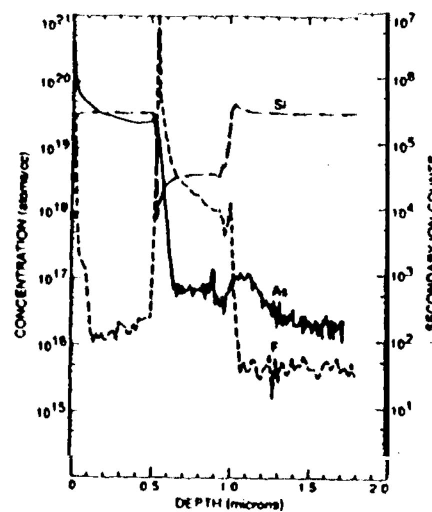

POCL DOPED **As IMPLANT**

Figure 2. Elemental Distribution as a Function of Depth from Surface.

Diffraction profile shape analysis of the (001) from the polysilicon layer of both the $POCl_3$ and the arsenic doped gave a average diffracting particle size of 29nm and a particle size distribution function shown in Fig. 3. The range of sizes observed are from 16 to 34nm with the mode of the distribution function at 25nm. These sizes are about one twentieth of the thickness of the polysilicon deposited film which correlates well with the cross-sectional TEM observations (see Fig. I).

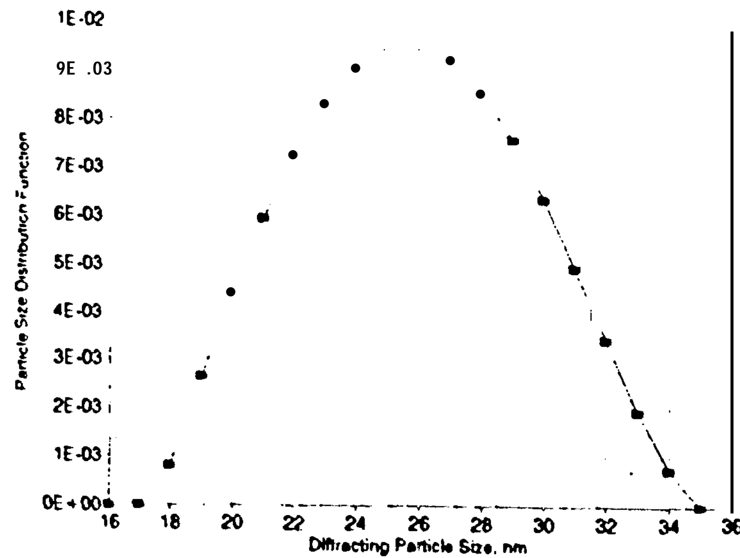

Figure 3. Diffracting Particle Distribution Function for Arsenic Doped 480nm Thick Sample

Stress in the Multilayer Structures

Synchrotrons Measurements:

The stress determinations were done by a two tilt method employing tilt angles of 30 and 60 degrees for $POCl_3$ and 26 and 48 degrees for arsenic doped samples. The axial system in which the strain calculations were done were the crystal axial system because there exits a strong (001) texture. The elastic constants of silicon used in the calculations were $c_{11} = 16.74X10^{11}$, $c_{12}=6.52X10^{11}$ and $c_{44}=7.96X10^{11}$ dynes/cm^2 (15). The polysilicon film stresses are reported in Table II.

X-Ray Rocking Curve Measurements:

The shift of the (400) peak from the substrate silicon as a function of horizontal displacement is shown in Fig. 4. The stresses determined from the curvature measurements are shown in Table IL The magnitude of the film stresses determined from the substrate curvatures consistently higher than the stresses in the films calculated from the double tilt data obtained on beamline X14 at NSLS.

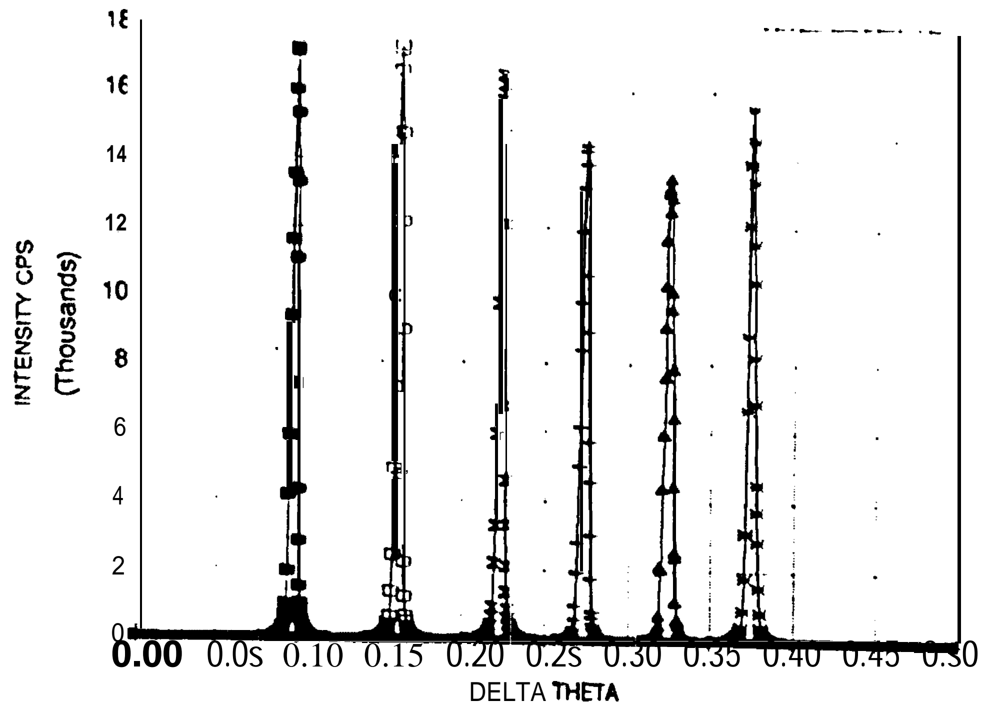

Figure 4. X-Ray Rocking curves from Processed Wafer.

Stress Gradients in Oxide Layer:

The stress gradients in the oxide layers were estimated by assuming that the stress in the polysilicon layer extends to the silica interface and the stress in the film determined from the substrate curvature also exists at the silica interface Then an estimate of the stress gradient in the oxide layer can be estimated, as shown in Fig.5, by assuming a linear gradient through the oxide. These gradients, in MPa per micron, are shown in Table II. As can be easily seen the stress gradients that were estimated for the arsenic doped structures were generally much steeper than the $POCl_3$ doped or no doped specimens.

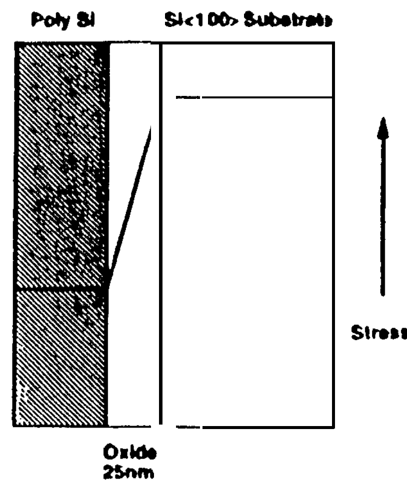

Figure 5. Method Employed to Estimate the Oxide Stress Gradient.

TABLE II: Estimation of the Stress Gradients in SiO_2 Layers

DOPANT-THICK-F 10N DOSE PER CM^{-2}	POLYSILICON STRESS MPa	FILM STRESS SUBSTRATE CURVATURE MPa	SiO_2 STRESS GRADIENT PER UNIT THICKNESS
As-480nm-NO	214	554	13.6
As-480nm-6E15	215	684	18.7
As-270nm-NO	-129	-993	34.5
As-270nm-6E15	128	174	1.8
P-830nm-NO	-68	-77	0.36
P-830nm-6E15	136	290	6.2
P-270nm-NO	44	88	1.8
P-270nm-6E15	-160	-253	3.7
NONE-480nm-NO	179	383	8.2

Electrical Performance

The linear region of the transconductance degradation at 300K and 77K for both the control and the fluorinate $POCl_3$ doped devices are shown in Fig.6. At room temperature the fluorine incorporation results in a 300% improvement.

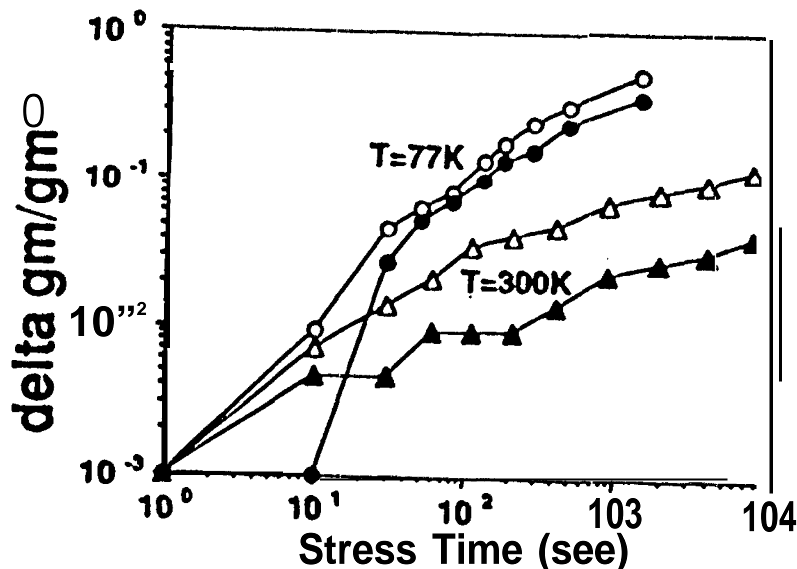

Figure 6. The Effects of Fluorine Incorporation on Hot Carrier Lifetime

The same tests performed on the arsenic doped samples showed lifetimes similar to the non-fluorinated $POCl_3$ doped devices and no improvement was observed with fluorination. In general, as the N_{it} increases the hot carrier lifetime decreases, due to a grater density of carrier trap sites (14). Therefore, in general, a lower film stress should improve the hot carrier lifetime, The experimental stress measurements do not support this, the fluorine incorporation in the $POCl_3$ typically increased the film stresses, The arsenic doped samples showed no increase in film stress after fluorine incorporation. The incorporation of fluorine appeared to have no effect on the magnitude of the estimated stress gradients,

A high fluorine concentration gradient was observed in the arsenic doped samples, these samples also had higher polysilicon film stress and greater stress gradients through the oxide layer. The stress gradient may be inhibiting the fluorine diffusion through the oxide layer where 8it could interact with the dangling bonds at the oxide/substrate interface. If the improvements in electrical performance are due to physical modifications occurring in the oxide as a result of the fluorine implantation, this would suggest that the stress state and microstructure in the arsenic doped samples may be preventing this beneficial effect.

Based on this investigation it is concluded that; the dopant had a substantial effect on the polysilicon film stress and microstructure. However, the fluorine implantation appears to have no effect on either the film stress or the stress gradient through the oxide.

ACKNOWLEDGEMENTS :

This investigation was partially supported by funds from the National Science Foundation on EPSCoR Grant No: NSF-OSR-95255225. The portion of this research that was performed at the Oak Ridge National Laboratory beamline X-14 at the Brookhaven National Laboratory is sponsored by the U, S. Department of Energy under contract No: DE-AC05-84OR21 400 with the Martin Marietta Energy Systems, Inc.

REFERENCES:

1. Y. Nishioka et al.; IEEE Electron Device Letters; 9 (1988) 38.

2. P. J. Wright et al.; IEEE Trans. Electron Devices; 36 (1989) 879.

3. K. P. MacWillians, L. E, Lowry; IEEE Electron Devices; 11 (1990) 3,

4. S, M, Sze; “VLSI Technology”; McGraw-Hill Book Co., New York (1988) 481.

5. G. Bai and M-A Nicolet; “Defect Production in Si(1 00) by ^{19}F, ^{28}Si, Ar and ^{131}Xe Implantation at Room Temperature”; J. Appl.Phys; 70 (1991) 3551.

6. G. Bai; Private Communication.

7. Paul A. Flinn and Chien Chiang; “X-Ray Diffraction Determination of the Effect of Various Passivations on Stress in Metal Films and Patterned Lines”; J, Appl. Phys., 67 (1990) 2927, ”

8. H. K. Kuo, P. Ganesan and R. J. De Angel is, “A Method to Study Sintering of A Supported Metal Catalysts”, Microstructural Science, 8 (1980) 311,

9. P. Ganesan, A. Saavedra and R. J. De Angelis; “Particle Size Distribution Function of Supported Metal Catalysts by X- ray Diffraction”; J. Catalysis, 52 (1978) 310.

10. T Vreeland, Jr. and B. M. Paine; Vat. Sci. Technol. A; 4 (1986) 3153.

11. T. Vreeland, Jr. A. Dommann, C. J. Tsai and M-A. Nicolet; Mat. Res. Sot. Symp. Proc.; 130 (1 989) 3.

12. G. G. Stoney, Proc. Roy. Sot. A (London), 46 (1969) 172.

13. I. C. Noyan and C. C. Goldsmith; “A Comparative Study of Stress Determination Techniques in Polycrystalline Thin Films”; Adv. X-Ray Anal.; 33 (1990) 137,

14. F. J. Grunthaner, P. J. Grunthaner and J. Maserjian; IEEE Trans. Nut. Sot.; 29 (1982) 1462.

15. Helmut F. Wolf; “Semiconductors”; Publisher Wiley-Interscience, New York; 1971; p. 128.